ijndes
Published by Global Research Publications, New Delhi, India

CONTROLLING HOPF BIFURCATION OF SSR AS APPLIED TO MULTIMACHINE POWER SYSTEM

Majdi M. Alomari and Benedykt S. Rodanski
University of Technology, Sydney (UTS), P.O. Box 123, Broadway NSW 2007, Australia

Received: 13th May 2016, Accepted: 12th September2016

Abstract: *This paper introduces the use of nonlinear controller to convert the unstable periodic solution to a stable one. The idea is altering the subcritical Hopf bifurcation to supercritical. The second system of the IEEE second benchmark model of Subsynchronous Resonance (SSR) is considered. The system can be mathematically modeled as a set of first order nonlinear ordinary differential equations with the compensation factor ($\mu = X_c/X_L$) as a control parameter. Therefore, bifurcation theory can be applied to nonlinear dynamical systems, which can be written as $dx/dt=F(x;\mu)$. The dynamics of the damper winding, automatic voltage regulator (AVR), and power system stabilizer (PSS) on SSR in power system are included. Nonlinear state feedback controller (Static Feedback Controller) with a form of $u = -K(\omega_{r1}{}^3 - \omega_1{}^3)$ can be used together with a small AVR gain to stabilize the system. It requires measurements in only two state variables. On the other hand, based on bifurcation theory and center manifold theory, a nonlinear controller is used to control a Hopf bifurcation and chaos.*

Keywords: *Bifurcation Theory, Nonlinear Controller, Center Manifold.*

1. INTRODUCTION

Power systems have rich bifurcation phenomena. Recently, power system dynamics has been studied using the nonlinear dynamics point of view, which utilizes the bifurcation theory. Bifurcation is used to indicate a qualitative change in the features of a system, such as the number and types of solution upon a small variation in the parameters of a system. The objectives of typical bifurcation control are: introducing a new bifurcation at preferable parameter value, delaying the onset of an inherent bifurcation, stabilizing a bifurcation solution or branch, modifying the shape or type of a bifurcation chain, changing the parameter value of an existing bifurcation point, optimizing the system performance near a bifurcation point and monitoring the multiplicity, amplitude and frequency of some limit cycles emerging from bifurcation.

The concept of bifurcation control has many practical applications in various science fields. These include chemical engineering, mechanical engineering, electrical engineering, biology, physics and chemistry and meteorology. There are several feedback control methods

which can be used to adjust bifurcation properties. Such methods utilize linear or nonlinear state feedback controls, harmonic balance approximations, and a washout filter-aided dynamic feedback controller.

In power systems series compensation is considered as a powerful technique based on economic and technical considerations for increasing effectively the power transfer capability as well as improving the stability of these systems. However, this introduces problems as well as with the benefits, namely the electromechanical interaction between electrical resonant circuits of the transmission system and the torsional natural frequencies of the turbine-generator rotor. This phenomenon is called subsynchronous resonance (SSR), and it can cause shaft fatigue and possible damage or failure. SSR has been studied extensively since 1970, when a major transmission network in southern California experienced shaft failure to its turbine-generator unit with series compensation. The phenomenon of subsynchronous resonance occurs mainly in series capacitor-compensated transmission systems.

The objectives of typical bifurcation control are: introducing a new bifurcation at preferable parameter value [1 and 2], delaying the onset of an inherent bifurcation [3 and 4], stabilizing a bifurcation solution or branch [5 and 6], modifying the shape or type of a bifurcation chain [4], changing the parameter value of an existing bifurcation point [7 and 8], optimizing the system performance near a bifurcation point [9] and monitoring the multiplicity [10], amplitude [11] and frequency of some limit cycles emerging from bifurcation [12].

Tomim et al. [13] proposed an index that identifies Hopf bifurcation points in power systems susceptible to subsynchronous resonance. Abed and Fu [14 and 15] illustrated how the static feedback controller u can be chosen to suppress discontinuous bifurcations of fixed points such as subcritical Hopf bifurcations. They showed that subcritical Hopf bifurcation is converted to supercritical Hopf bifurcation by using a nonlinear static feedback. Nayfeh *et. al*. [16] used a nonlinear state feedback controller in the form of $u=Kx^3$ to change the subcritical to a supercritical Hopf bifurcation.

Also, they used this controller to reduce the amplitude of the limit cycle born near the bifurcation value as the controller gain value increases. Shahrestani and Hill [17] used a linear controller to delay the inception of a bifurcation. Furthermore, they showed that when the critical modes are not controllable or when the control objective is set as the stabilization of periodic solutions, nonlinear controller must be considered. They also derived control laws utilizing nonlinear feedback of critical states.

In this study, we use bifurcation theory and center manifold theory to investigate the complex dynamics of the considered system. The type of the Hopf bifurcation is determined by numerical integration of the system, with specific amount of initial disturbances, slightly before and after the bifurcation value. On further increase of the compensation factor, the system experiences chaos via torus attractor. Chaos is a bounded steady-state behavior that is not an equilibrium solution or a periodic solution or a quasiperiodic solution [18]. We focus on the torsional interaction effect, which results from the interaction of the electrical subsynchronous mode with the torsional mode.

2. SYSTEM DESCRIPTION

The system considered is the two different machine infinite bus system, shown in Figure 1. The two machines have a common torsional mode connected to a single series compensated transmission line. The model and the parameters are provided in the second system of the IEEE second benchmark model. The electro-mechanical systems for the first and second units are shown in Figure 2. The first unit consists of exciter (EX.), generator (Gen.1), low-pressure (LP1) and high-pressure (HP1) turbine sections. And the second unit consists of generator (Gen.2), low-pressure (LP2) and high-pressure (HP2) turbine sections. Every section has its own angular momentum constant M and damping coefficient D, and every pair of successive masses have their own shaft stiffness constant K, as shown in Figure 2. The data for electrical and mechanical system are provided in [19]. Replacement of these generators with a single equivalent generator will change the resonance characteristics and therefore is not justified. Consequently, each generator is represented in its own rotor frame of reference and suitable transformation is made.

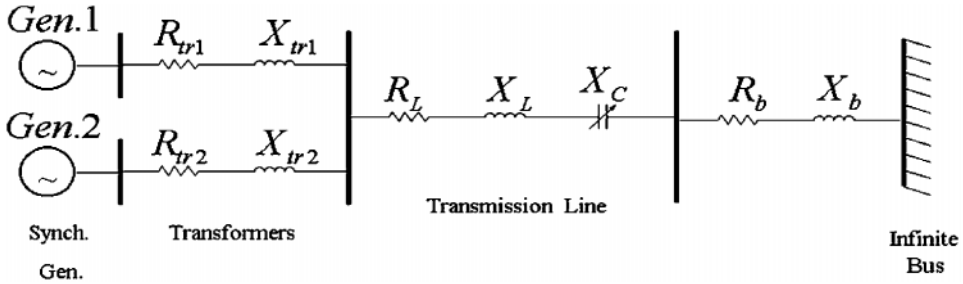

Figure 1: Electrical System (Two different Machine Infinite Bus System)

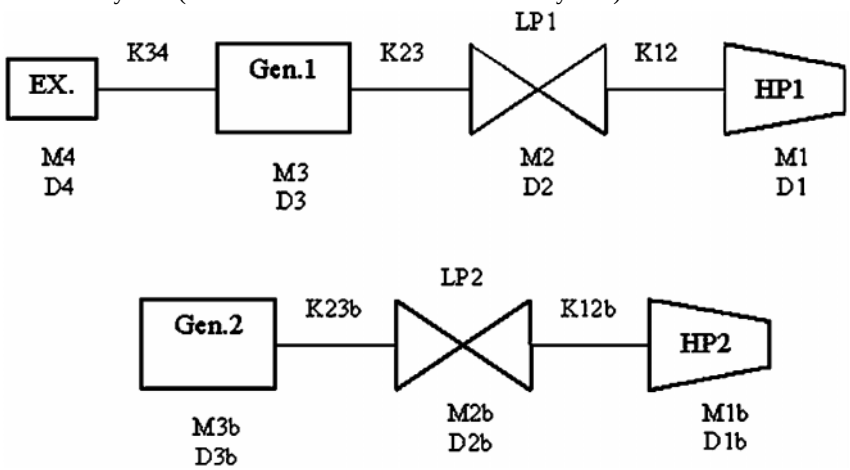

Figure 2: Electro-mechanical Systems for the First and Second Units

3. MATHEMATICAL MODEL

The mathematical model of the electrical and mechanical system will be presented in this section. Actually, the electrical system includes the dynamic nonlinear mathematical model of a synchronous generator and that of the transmission line. The generator model considered in

this study includes five equations, *d*-axis stator winding, *q*- axis stator winding, d-axis rotor field winding, q-axis rotor damper winding and d-axis rotor damper winding equations. Each mass of the mechanical system can be modeled by a second order ordinary differential equation (swing equation), which is presented in state space model as two first order ordinary differential equations [20]. Using the direct and quadrature *d-q* axes and Park's transformation, we can write the complete mathematical model that describes the dynamics of the system as follows:

Generator # 1:

$$
\begin{aligned}
&-(X_{tr1}+X_L+X_b+X_{d1})\frac{di_{d1}}{dt}-(X_L+X_b)\cos\delta_{r12}\frac{di_{d2}}{dt}-(X_L+X_b)\sin\delta_{r12}\frac{di_{q2}}{dt}\\
&+X_{md1}\frac{di_{f1}}{dt}+X_{md1}\frac{di_{D1}}{dt}=\omega_b\left\{(R_{tr1}+R_L+R_b+R_{a1})i_{d1}+\left[(R_L+R_b)\cos\delta_{r12}\right.\right.\\
&\left.+(\frac{\omega_{r2}}{\omega_b}+1)(X_L+X_b)\sin\delta_{r12}\right]i_{d2}-\left[\frac{\omega_{r1}}{\omega_b}(X_{tr1}+X_L+X_b)+(X_L+X_b)+\omega_{r1}X_{q1}\right]i_{q1}\\
&+\left[(R_L+R_b)\sin\delta_{r12}-(\frac{\omega_{r2}}{\omega_b}+1)(X_L+X_b)\cos\delta_{r12}\right]i_{q2}+X_{mq1}\omega_{r1}i_{Q1}\\
&\left.+e_{cd}\sin\delta_{r1}-e_{cq}\cos\delta_{r1}+V_{0D}\sin\delta_{r1}-V_{0Q}\cos\delta_{r1}\right\}
\end{aligned}
\tag{1}
$$

$$
\begin{aligned}
&-(X_{tr1}+X_L+X_b+X_{q1})\frac{di_{q1}}{dt}-(X_L+X_b)\cos\delta_{r12}\frac{di_{q2}}{dt}+(X_L+X_b)\sin\delta_{r12}\frac{di_{d2}}{dt}\\
&+X_{mq1}\frac{di_{Q1}}{dt}=\omega_b\left\{(R_{tr1}+R_L+R_b+R_{a1})i_{q1}+\left[(R_L+R_b)\cos\delta_{r12}\right.\right.\\
&\left.+(\frac{\omega_{r2}}{\omega_b}+1)(X_L+X_b)\sin\delta_{r12}\right]i_{q2}+\left[\frac{\omega_{r1}}{\omega_b}(X_{tr1}+X_L+X_b)+(X_L+X_b)+\omega_{r1}X_{d1}\right]i_{d1}\\
&+\left[-(R_L+R_b)\sin\delta_{r12}+(\frac{\omega_{r2}}{\omega_b}+1)(X_L+X_b)\cos\delta_{r12}\right]i_{d2}-X_{md1}\omega_{r1}i_{f1}\\
&\left.-X_{md1}\omega_{r1}i_{D1}+e_{cd}\cos\delta_{r1}+e_{cq}\sin\delta_{r1}+V_{0D}\cos\delta_{r1}+V_{0Q}\sin\delta_{r1}\right\}
\end{aligned}
\tag{2}
$$

$$
-X_{md1}\frac{di_{d1}}{dt}+X_{f1}\frac{di_{f1}}{dt}+X_{md1}\frac{di_{D1}}{dt}=\omega_b\left[-R_{f1}i_{f1}+\frac{R_{f1}E_{fd1}}{X_{md1}}\right] \tag{3}
$$

$$
-X_{mq1}\frac{di_{q1}}{dt}+X_{Q1}\frac{di_{Q1}}{dt}=-\omega_b R_{Q1}i_{Q1} \tag{4}
$$

$$
-X_{md1}\frac{di_{d1}}{dt}+X_{md1}\frac{di_{f1}}{dt}+X_{D1}\frac{di_{D1}}{dt}=-\omega_b R_{D1}i_{D1} \tag{5}
$$

where: $v_{f1}=\dfrac{R_{f1}E_{fd1}}{X_{md1}}$

$i\ ,\ j=1\ ,\ 2\quad and\quad i\neq j\ ,\quad \sin\delta_{rij}=\sin\ (\delta_{ri}-\delta_{rj})\ ,\quad \cos\delta_{rij}=\cos\ (\delta_{ri}-\delta_{rj})$

Similarly, for the second generator the generator model includes five equations as follows:

$$\begin{aligned}
&-(X_{tr2}+X_L+X_b+X_{d2})\frac{di_{d2}}{dt}-(X_L+X_b)\cos\delta_{r21}\frac{di_{d1}}{dt}-(X_L+X_b)\sin\delta_{r21}\frac{di_{q1}}{dt}\\
&+X_{md2}\frac{di_{f2}}{dt}+X_{md2}\frac{di_{D2}}{dt}=\omega_b\left\{(R_{tr2}+R_L+R_b+R_{a2})i_{d2}+\left[(R_L+R_b)\cos\delta_{r21}\right.\right.\\
&+\left(\frac{\omega_{r1}}{\omega_b}+1\right)(X_L+X_b)\sin\delta_{r21}\left.\right]i_{d1}-\left[\frac{\omega_{r2}}{\omega_b}(X_{tr2}+X_L+X_b)+(X_L+X_b)+\omega_{r2}X_{q2}\right]i_{q2}\\
&+\left[(R_L+R_b)\sin\delta_{r21}-\left(\frac{\omega_{r1}}{\omega_b}+1\right)(X_L+X_b)\cos\delta_{r21}\right]i_{q1}+X_{mq2}\omega_{r2}i_{Q2}\\
&\left.+e_{cd}\sin\delta_{r2}-e_{cq}\cos\delta_{r2}+V_{0D}\sin\delta_{r2}-V_{0Q}\cos\delta_{r2}\right\}
\end{aligned} \tag{6}$$

$$\begin{aligned}
&-(X_{tr2}+X_L+X_b+X_{q2})\frac{di_{q2}}{dt}-(X_L+X_b)\cos\delta_{r21}\frac{di_{q1}}{dt}+(X_L+X_b)\sin\delta_{r21}\frac{di_{d1}}{dt}\\
&+X_{mq2}\frac{di_{Q2}}{dt}=\omega_b\left\{(R_{tr2}+R_L+R_b+R_{a2})i_{q2}+\left[(R_L+R_b)\cos\delta_{r21}\right.\right.\\
&+\left(\frac{\omega_{r1}}{\omega_b}+1\right)(X_L+X_b)\sin\delta_{r21}\left.\right]i_{q1}+\left[\frac{\omega_{r2}}{\omega_b}(X_{tr2}+X_L+X_b)+(X_L+X_b)+\omega_{r2}X_{d2}\right]i_{d2}\\
&+\left[-(R_L+R_b)\sin\delta_{r21}+\left(\frac{\omega_{r1}}{\omega_b}+1\right)(X_L+X_b)\cos\delta_{r21}\right]i_{d1}-X_{md2}\omega_{r2}i_{f2}\\
&\left.-X_{md2}\omega_{r2}i_{D2}+e_{cd}\cos\delta_{r2}+e_{cq}\sin\delta_{r2}+V_{0D}\cos\delta_{r2}+V_{0Q}\sin\delta_{r2}\right\}
\end{aligned} \tag{7}$$

$$-X_{md2}\frac{di_{d2}}{dt}+X_{f2}\frac{di_{f2}}{dt}+X_{md2}\frac{di_{D2}}{dt}=\omega_b\left[-R_{f2}i_{f2}+\frac{R_{f2}E_2}{X_{md2}}\right] \tag{8}$$

$$-X_{mq2}\frac{di_{q2}}{dt}+X_{Q2}\frac{di_{Q2}}{dt}=-\omega_b R_{Q2}i_{Q2} \tag{9}$$

$$-X_{md2}\frac{di_{d2}}{dt}+X_{md2}\frac{di_{f2}}{dt}+X_{D2}\frac{di_{D2}}{dt}=-\omega_b R_{D2}i_{D2} \tag{10}$$

where : $v_{f2}=\dfrac{R_{f2}E_2}{X_{md2}}$

Voltage drop across *Xc*:

$$\frac{de_{cd}}{dt}=\omega_b[X_cI_{LD}+e_{cq}] \tag{11}$$

$$\frac{de_{cq}}{dt}=\omega_b[X_cI_{LQ}-e_{cd}] \tag{12}$$

where : $I_{LD} = I_{q1}\cos\delta_1 + I_{q2}\cos\delta_2 + I_{d1}\sin\delta_1 + I_{d2}\sin\delta_2$

$I_{LQ} = I_{q1}\sin\delta_1 + I_{q2}\sin\delta_2 - I_{d1}\cos\delta_1 - I_{d2}\cos\delta_2$

Mechanical System:

High-pressure turbine # 1:

$$\frac{d\omega_1}{dt} = \frac{1}{M_1}\left[-D_1(\omega_1 - 1) - K_{12}(\theta_1 - \theta_2)\right] \tag{13}$$

$$\frac{d\theta_1}{dt} = \omega_b(\omega_1 - 1) \tag{14}$$

Low-pressure turbine # 1:

$$\frac{d\omega_2}{dt} = \frac{1}{M_2}\left[-D_2(\omega_2 - 1) + K_{12}(\theta_1 - \theta_2) - K_{23}(\theta_2 - \delta_{r1})\right] \tag{15}$$

$$\frac{d\theta_2}{dt} = \omega_b(\omega_2 - 1) \tag{16}$$

Similarly, for the second High- and low-pressure turbine:

High-pressure turbine # 2:

$$\frac{d\omega_{1b}}{dt} = \frac{1}{M_{1b}}\left[-D_{1b}(\omega_{1b} - 1) - K_{12b}(\theta_{1b} - \theta_{2b})\right] \tag{17}$$

$$\frac{d\theta_{1b}}{dt} = \omega_b(\omega_{1b} - 1) \tag{18}$$

Low-pressure turbine # 2:

$$\frac{d\omega_{2b}}{dt} = \frac{1}{M_{2b}}\left[-D_{2b}(\omega_{2b} - 1) + K_{12b}(\theta_{1b} - \theta_{2b}) - K_{23b}(\theta_{2b} - \delta_{r2})\right] \tag{19}$$

$$\frac{d\theta_{2b}}{dt} = \omega_b(\omega_{2b} - 1) \tag{20}$$

Generator # 1:

$$\frac{d\omega_{r1}}{dt} = \frac{1}{M_3}\left[T_{m1} - T_{e1} + K_{23}(\theta_2 - \delta_{r1}) - K_{34}(\delta_{r1} - \theta_4) - D_3(\omega_{r1} - 1)\right] \tag{21}$$

$$\frac{d\delta_{r1}}{dt} = \omega_b(\omega_r - 1) \tag{22}$$

where: $T_{e1} = i_{q1}\Psi_{d1} - i_{d1}\Psi_{q1}$

$= (X_{q1} - X_{d1})i_{d1}i_{q1} + X_{md1}i_{f1}i_{q1} - X_{mq1}i_{Q1}i_{d1} + X_{md1}i_{D1}i_{q1}$

Generator # 2:

$$\frac{d\omega_{r2}}{dt} = \frac{1}{M_{3b}}\left[T_{m2} - T_{e2} + K_{23b}(\theta_{2b} - \delta_{r2}) - D_{3b}(\omega_{r2} - 1)\right] \tag{23}$$

$$\frac{d\delta_{r2}}{dt} = \omega_b(\omega_{r2} - 1) \quad (24)$$

where: $T_{e2} = i_{q2}\Psi_{d2} - i_{d2}\Psi_{q2}$

$$= (X_{q2} - X_{d2})i_{d2}i_{q2} + X_{md2}i_{f2}i_{q2} - X_{mq2}i_{Q2}i_{d2} + X_{md2}i_{D2}i_{q2}$$

Exciter:

$$\frac{d\omega_4}{dt} = \frac{1}{M_4}\left[-D_4(\omega_4 - 1) + K_{34}(\delta_{r1} - \theta_4)\right] \quad (25)$$

$$\frac{d\theta_4}{dt} = \omega_b(\omega_4 - 1) \quad (26)$$

The mathematical models of AVR and PSS (shown in Figure 3) can be written as follows:

$$\frac{d\omega_{r1}}{dt} - \frac{dX_{W1}}{dt} = \frac{1}{T_W}X_{W1} \quad (27)$$

$$K_s T_1 \frac{dX_{W1}}{dt} - T_2 \frac{dV_{S1}}{dt} = V_{s1} - K_s X_{W1} \quad (28)$$

$$T_R \frac{dE_1}{dt} = K_R(V_{ref1} + V_{S1} - V_{t1}) - E_1 \quad (29)$$

Where : $V_{t1} = \sqrt{V_{d1}^2 + V_{q1}^2}$

Neglecting stator transients yields:

$$V_{d1} = -R_{a1}i_{d1} + X_{q1}i_{q1}$$

$$V_{q1} = -R_{a1}i_{q1} - X_{d1}i_{d1} + X_{md1}i_{fd1}$$

Consequently, $V_{t1} = \sqrt{(-R_{a1}i_{d1} + X_{q1}i_{q1})^2 + (-R_{a1}i_{q1} - X_{d1}i_{d1} + X_{md1}i_{fd1})^2}$ (30)

Therefore, these systems can be mathematically modeled as a set of first order nonlinear ordinary differential equations with the compensation factor ($\mu = X_c/X_L$) as a bifurcation (control) parameter. So, bifurcation theory can be applied to nonlinear dynamical systems, which can be written in the form $dx/dt=F(x; \mu)$.

4. SYSTEM RESPONSE WITHOUT CONTROLLER

In this section we investigate the case of adding damper windings, automatic voltage regulator (AVR) and power system stabilizer (PSS) to the first generator. Figure 3 shows the block diagram of the use of AVR together with the PSS [21].

The operating point stability regions in the δ_{r1} plane together with two Hopf bifurcation points are depicted in Figure 4. We observe that the power system has a stable operating point to the left of $H_1 \approx 0.198377$and to the right of $H_2 \approx 0.824135$, and has an unstable operating point between H_1 and H_2. The operating point loses stability at a Hopf bifurcation point, namely $\mu = H_1$. It regains stability at a reverse Hopf bifurcation, namely $\mu = H_2$.

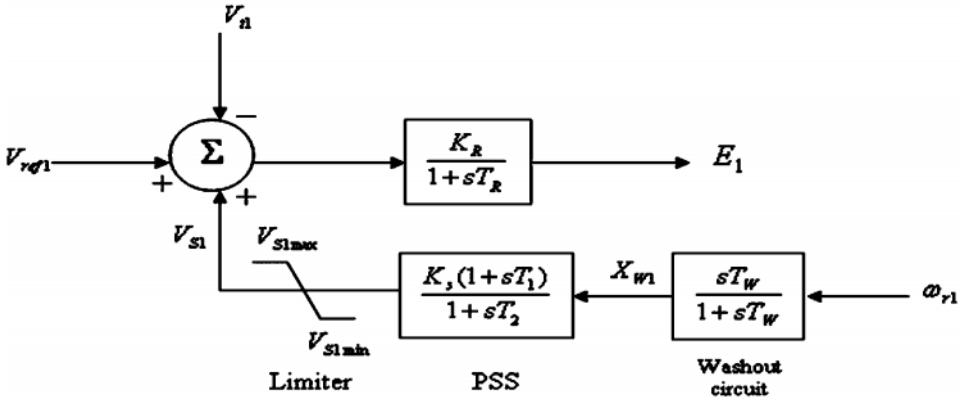

Figure 3: Block Diagram of the use of AVR and PSS to the First Generator

In this case a pair of complex conjugate eigenvalues will transversally cross from left half to right half of the complex plane, and then back to the left half. To determine whether the limit cycles created due to the Hopf bifurcation are stable or unstable, we obtain the time response . Figure 5 shows the response of the system with 7% initial disturbance on the speed of the generator at $\mu = 0.182265$, which is less than H_1. It can be observed that the system is unstable. Therefore, the type of this Hopf bifurcation is subcritical. So, the periodic solution emanating at the bifurcation point is unstable.

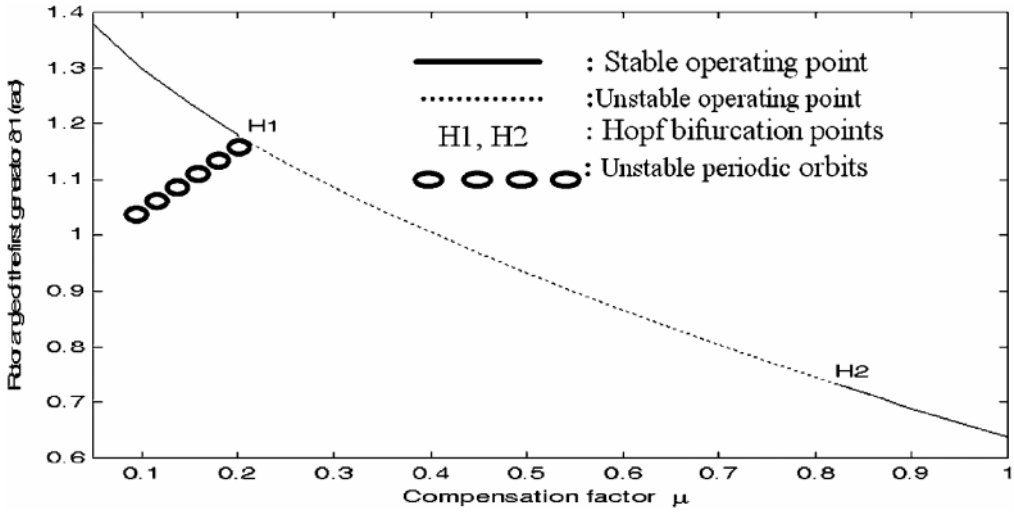

Figure 4: Bifurcation Diagram Showing Variation of the First Generator Rotor Angle δ_{r1} with the Compensation Factor μ (for the Case of no Controller).

5. CONTROL OF HOPF BIFURCATION AND CHAOS

Consider the nonlinear dynamical system presented in the form:

$$\dot{x} = f(x,u;\mu)$$
$$y = g(x) \qquad (31)$$

Where x is a state variables vector, f is the field vector, μ is the control parameter of the system, y is the system outputs and u is the system state feedback control inputs. At any value of compensation factor μ, the operating points (equilibrium solutions) are obtained by setting the derivatives of the state variables in the system equal to zero.

$$f(x_e, u_e; \mu) = 0 \tag{32}$$

Where u_e represents the control input value when the system is at the equilibrium. The stability of the equilibrium solution is studied by examination of the eigenvalues of the Jacobian matrix evaluated at the operating point. Consider the system undergoing a Hopf bifurcation at the considered equilibrium point. That is, the critical eigenvalues of A cross imaginary axis at $\pm j\beta$, while all other eigenvalues have strictly negative real part. In this study, the case of including the dynamics of the two axes damper windings, AVR and PSS is considered.

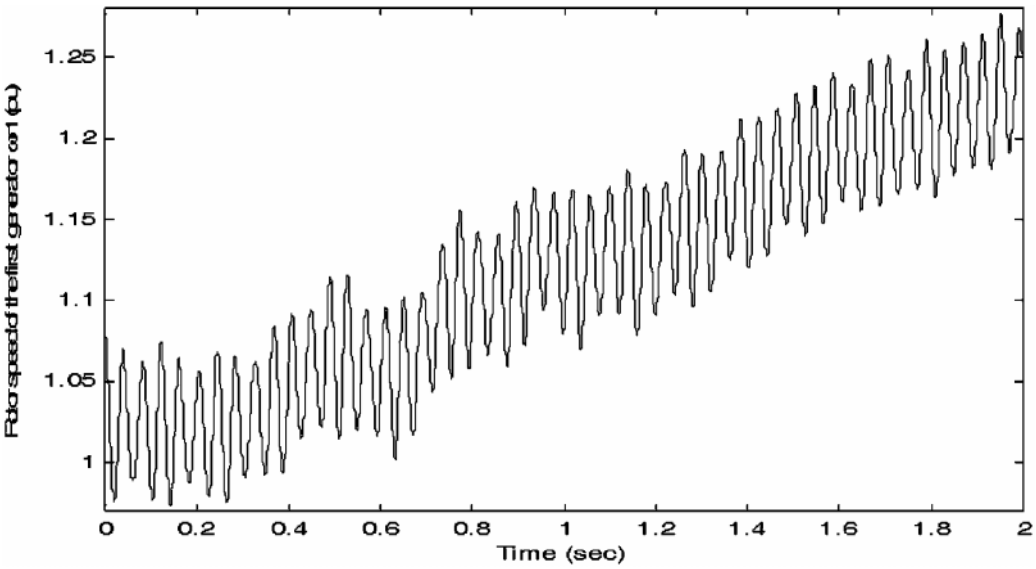

Figure 5: Rotor Speed of the Generator at μ = 0.182265 with 7% Initial Disturbance in Rotor Speed of Generator (for the Case of no Controller).

5.1. Nonlinear State Feedback Controller (Static Feedback Control)

The state feedback controller law in this method is nonlinear. It is used to achieve desirable nonlinear dynamics. This type of controller has been utilized by Nayfeh *et al.* [22].

For instance, consider the nonlinear dynamical system presented in the form:

$$\dot{x} = F(x; \mu) + u \tag{33}$$

Based on the nonlinearity of the system and by using trial and error criterion, we consider a nonlinear controller of the form:

$$u = -K(\omega_{r1}^{\ 3} - \omega_1^{\ 3}) \tag{34}$$

Figure 6 shows the block diagram of the AVR, PSS together with the considered nonlinear controller.

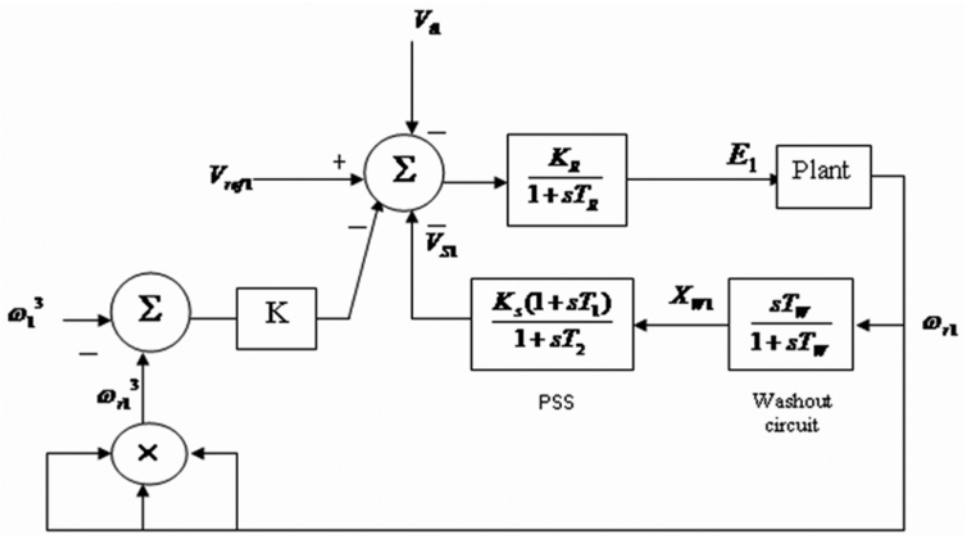

Figure 6: Block Diagram of the AVR, PSS Together with the Considered Nonlinear Controller

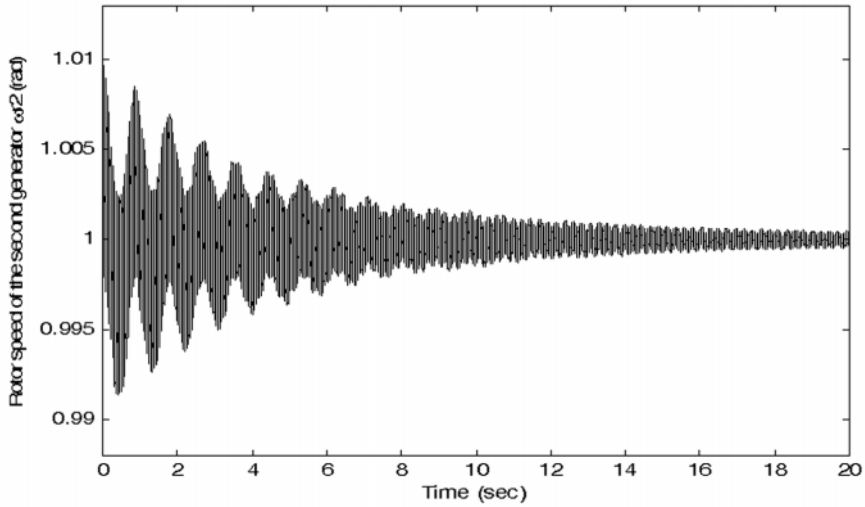

Figure 7: Rotor Speed of the Generators at μ = 0.7 with 1% Initial Disturbance in Rotor Speed of Generators. (For the Case of Adding Damper Windings, AVR and PSS with Nonlinear State Feedback Controller with a Gain K = 6000 and the Nominal Value of AVR Gain K_R = 4).

In this study, the two state signals of the system: the rotor speed of the first generator ω_{r1} and the first turbine-generator section speed ω_1, must be measured. The result of subtraction of ω_1^3 from ω_{r1}^3 will be obtained. The nonlinear controller will not affect the equilibrium of the system because $\omega_{r1} = \omega_1$ at steady state. But it will affect the Jacobian matrix of the system, as a result, the eigenvalues of the linearized model will change by this controller at different values of μ. Then, the result is multiplied by a gain K. This gain must be carefully adjusted such that it will make a significant effect on the equilibrium stability of the system. Figure 7 shows the system response after 1% initial disturbance in generator rotor speed at μ = 0.7 when the nonlinear state feedback controller is applied. It can be observed that, the nonlinear

controller with a gain K = 6000 together with a small value of AVR gain K_R = 4 stabilizes the system. The time history of the nonlinear controller u after 1% initial disturbance in generator rotor speed at μ = 0.7 is shown in Figure 8.

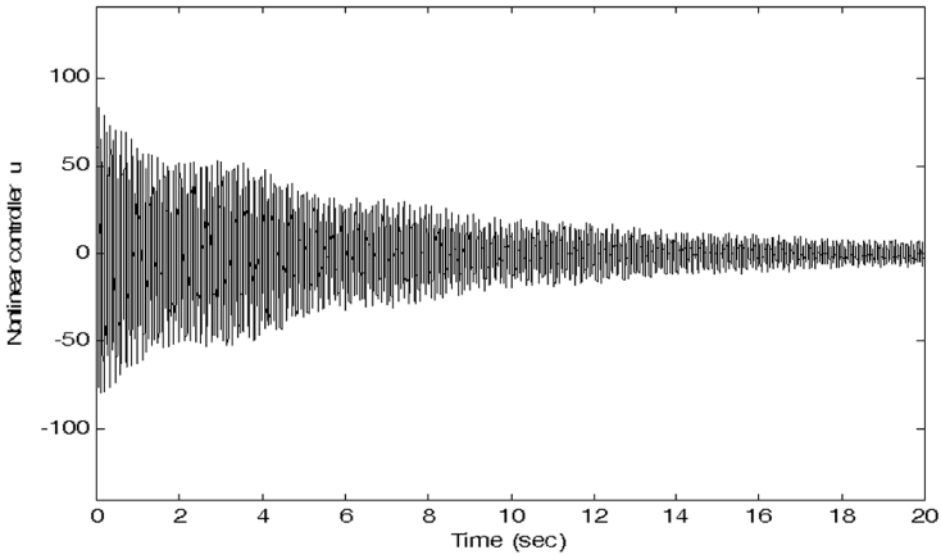

Figure 8: Nonlinear Controller u at μ = 0.7 after 1% Initial Disturbance in Rotor Speed of Generators with Nonlinear State Feedback Controller with a Gain K= 6000)

5.2. Control of Hopf Bifurcation

The bifurcation point is transferred to the origin via simple change of coordinates, with $m = \mu - \mu_o$ and $w = u - u_e$ [17]. By utilizing appropriate similarity linear transformations, the Jacobian is transformed to diagonal form, with a 2 × 2 block for the critical complex eigenvalues. The system can be expressed in the form:

$$\begin{aligned} \dot{x}_c &= J_c X_c + f_c(x_c, x_s, w; m) \\ \dot{x}_s &= J_s X_s + f_s(x_c, x_s, w; m) \end{aligned} \tag{35}$$

Where J_s is a matrix whose eigenvalues all have negative real parts (i.e., J_s is a stable matrix) and the matrix J_c has the form

$$J_c = \begin{bmatrix} 0 & -\beta \\ \beta & 0 \end{bmatrix} \tag{36}$$

The functions f_c, f_s and their derivatives vanish at the origin. By the center manifold theorem [23] it can be ascertain that in the vicinity of origin (i.e., x_s, m, w: small) a smooth invariant manifold $x_s = h(x_c, m, w)$ for (35) exists. This center manifold is tangent to the eigenspace of the linearized system J_c,with $h(0,m,w) = h'(0,m,w) = 0$. Substituting the manifold constraint into the first part of (35), the bifurcation equations can be obtained as:

$$\dot{x}_c = J_c x_c + f_c(x_c, h(x_c, m, w), m, w) \tag{37}$$

For the purpose of notational simplicity, let $x_c = \begin{bmatrix} x & z \end{bmatrix}^T$, the bifurcation equations can now be considered as:

$$\dot{x} = f(x,z,m;w), \qquad \dot{z} = g(x,z,m;w) \tag{38}$$

Where $f(0,0,m,w)=g(0,0,w,m)=0$, and the Jacobian evaluated near the origin with $m = 0$, is J_c given by (36). The control w is of feedback type with $w(0,0) = 0$. Applying the Taylor expansion of (38) results in:

$$\begin{aligned} \dot{x} &= \left(f_{mx}m + f_w w_x\right)x - \left(\beta - f_w w_z - f_{mz} - f_{mz}m\right)z \\ \dot{z} &= \left(\beta + g_w w_x + g_{mx}m\right)x + \left(g_{mz}m + g_w w_z\right)z \end{aligned} \tag{39}$$

The characteristic polynomial of the Jacobian matrix can be obtained as:

$$\begin{aligned} &\lambda^2 - \lambda\left[f_w w_x + g_w w_z + m\left(f_{mx} + g_{mz}\right)\right] \\ &+\beta^2 - \beta\left[f_w w_z - g_w w_x + m\left(g_{mx} - f_{mz}\right)\right] \\ &-m\left[f_w\left(w_z g_{mx} - w_x g_{mz}\right) + g_w\left(w_x f_{mz} - w_z f_{mx}\right)\right] = 0 \end{aligned} \tag{40}$$

The roots of the characteristic polynomial are:

$$\lambda_{1,2}(m,w) = \alpha(m,w) \pm j\omega(m,w)$$

where:

$$\begin{aligned} \alpha(m,w) &= \frac{1}{2}\left[f_w w_x + g_w w_z + m\left(f_{mx} + g_{mz}\right)\right] \\ \omega(m,w) &= \beta - \frac{f_w w_z - g_w w_x - m\left(g_{mx} - f_{mz}\right)}{2} \\ &\quad + m\left[\frac{\left(f_{mx} - g_{mz}\right)\left(f_w w_x - g_w w_z\right) + 2\left(f_w w_z g_{mx} + g_w w_x f_{mz}\right)}{\beta}\right] \end{aligned} \tag{41}$$

In the case of no control effort (i.e. $w = 0$), the bifurcation parameter dependent eigenvalues can be evaluated as:

$$\lambda_{1,2}(m) = \frac{m}{2}\left(f_{mx} + g_{mz}\right) \pm j\left(\beta + \frac{m}{2}\left(g_{mx} - f_{mz}\right)\right) \tag{42}$$

Which has complex poles at $\pm j\beta$ for $m = 0$. The transversality condition requires that

$$\frac{d}{dm}\left[\mathrm{Re}\left(\lambda(m)\right)\right]_{m=0} \neq 0 \rightarrow \alpha_1 = \left(f_{mx} + g_{mz}\right) \neq 0 \tag{43}$$

Assume that the stability coefficient S be defined as:

$$\begin{aligned} S &= \frac{1}{16}\left(f_{xxx} + g_{xxz} + f_{xzz} + g_{zzz}\right) + \frac{1}{16}\left[f_{xz}\left(f_{xx} + f_{zz}\right)\right. \\ &\quad \left. -g_{xz}\left(g_{xx} + g_{zz}\right) - f_{xx}g_{xx} + f_{zz}g_{zz}\right] \end{aligned} \tag{44}$$

The Hopf bifurcation theorem establishes that in these circumstances, if the genericity condition $S\big|_{x=z=m=0} \neq 0$, is also satisfied a curve of periodic solutions bifurcates from the origin

into $m < 0$ provided $S\alpha_1$ is positive or into $m > 0$ if $S\alpha_1$ is negative. If α_1 is negative, the origin is stable for $m > 0$ and unstable for $m < 0$; conversely for α_1 positive, the origin is stable for $m<0$ and unstable for $m>0$. The periodic solutions on the side of $m = 0$ for which they exist, are stable if the origin is unstable and vice versa. On other words, for $\alpha_1 > 0$, a supercritical Hopf bifurcation occurs if $S<0$; the origin is stable for $m<0$ and unstable for $m>0$. As m passes through zero, the stable periodic solutions bifurcate into $m<0$. On the other hand, with α_1 positive, if $S>0$, the origin is stable and a subcritical Hopf bifurcation is displayed, with unstable periodic orbits bifurcating into $m<0$. In case of $\alpha_1<0$, situation is similar with the sign of m changed.

To study the possibility of rendering a subcritical Hopf bifurcation supercritical, the effects of control on S in (44) must also be investigated. For nonzero control effort, the new stability coefficient S_w to be evaluated at origin will be:

$$S_w = S + \frac{1}{16}\left[\left(w_{xxx} + w_{xzz}\right) f_w + \left(w_{zzz} + w_{xxz}\right) g_w\right] + \frac{1}{16\beta}\left[w_{xz}\left(f^2{}_w - g^2{}_w\right)\left(w_{xx} + w_{zz}\right) + f_w g_w\left(w^2{}_{zz} - w^2{}_{xx}\right)\right] \tag{45}$$

From S_w and $\lambda_{1,2}(m,w)$ it is clear that only the feedback of critical variables up to cubic terms, may have any effect on the existence of a Hopf bifurcation or changing its stability attitude. The elimination of subcritical bifurcation requires that $\acute{a}(m,w)$ in (41) be always negative. Nonlinear control (quadratic and/or cubic) can change the subcritical Hopf bifurcation to supercritical.

The quadratic feedback control law

$$w = k_1 x^2 + k_2 z^2 \tag{46}$$

Will change the subcritical Hopf bifurcation to supercritical, provided the critical modes are controllable and the feedback gains k_1 and k_2 are chosen such that

$$\frac{f_w g_w}{4\beta}(k_2{}^2 - k_1{}^2) < -S \tag{47}$$

Where S is defined by (44). The quadratic feedback will make the stability coefficient negative and hence changing the bifurcation to supercritical.

On the other hand, the cubic feedback control law

$$w = k_1 x^3 + k_2 z^3 \tag{48}$$

Will change the subcritical Hopf bifurcation to supercritical, where the feedback gains k_1 and k_2 are chosen such that

$$\frac{6}{16}(k_1 f_w + k_2 g_w) < -S \tag{49}$$

The cubic feedback will change the sign of the stability coefficient (45) resulting in a supercritical Hopf bifurcation.

For instance, consider the nonlinear dynamical system presented in the form:

$$\dot{x} = F(x;\mu) + u \tag{50}$$

To facilitate the use of previous results, the center manifold needs to be approximated. The new variables

$$y = V^{-1}.\delta x \tag{51}$$

are now introduced, where V is the transformation identified such that the Jacobian of

$$\dot{y} = V^{-1}.\dot{x} \tag{52}$$

evaluated near the bifurcation point is:

$$J = \begin{bmatrix} J_c & 0 \\ 0 & J_s \end{bmatrix} = \begin{bmatrix} 0 & -\beta & 0 & \cdots & \cdots & 0 \\ \beta & 0 & 0 & \cdots & \cdots & 0 \\ 0 & 0 & -|\lambda_1| & 0 & \cdots & 0 \\ \vdots & \vdots & 0 & \ddots & & \vdots \\ \vdots & \vdots & \vdots & & \ddots & 0 \\ 0 & 0 & 0 & \cdots & 0 & -|\lambda_{25}| \end{bmatrix} \tag{53}$$

Substituting the approximate center manifold constraint h in (35), it can be seen that it must satisfy the differential equation

$$h'(x_c)\cdot \dot{x}_c - \dot{x}_s = 0 \tag{54}$$

By utilizing the center manifold theorem and using (53), the bifurcation equations in the form of (37) can be identified. On the other hand, by using (43) and (44) α_1 is calculated to be 0.7426 and the stability coefficient S is 0.1235. So, for the control established by quadratic feedback of critical variables $w = k_1 x^2 + k_2 z^2$, the condition which is going to be achieved must be met will be

$$1.245(k_2^{\,2} - k_1^{\,2}) < -0.1235 \tag{55}$$

With $k_1 = 1$ and $k_2 = 0.25$, this will correspond to a negative value; resulting in stabilized oscillatory responses. Hence, the Hopf bifurcation will be changed from subcritical to supercritical. Figure 9 shows the system response after a 2% initial disturbance in generator rotor speed at $\mu = 0.401525$, which is greater than H_{1C}. It can be observed that the system routes to a periodic solution giving rise to oscillations. Hence, the type of this Hopf bifurcation is supercritical. So, the periodic solution emanating at the bifurcation point is stable. Figure 9 shows the system response after 2% initial disturbance in generator rotor speed at $\mu = H \approx 0.401525$ when the nonlinear (quadratic) controller is applied.

The same type of results in the quadratic feedback controller can be obtained by cubic feedback of critical variables $w = k_1 x^3 + k_2 z^3$. In this case, the condition that must be met will be

$$2.254k_1 + 3.165k_2 < -0.1235 \tag{56}$$

By choosing the feedback gains as $k_1 = 1$ and $k_2 = -0.8$, this coefficient will be negative to render the subcritical Hopf bifurcation supercritical. Figure 10 shows the system response after a 2% initial disturbance in generator rotor speed at $\mu = H \approx 0.401525$, which is greater than H_{1C}. It can be observed that the system routes to a periodic solution giving rise to oscillations. Hence, the type of this Hopf bifurcation is supercritical. So, the periodic solution emanating at

the bifurcation point is stable. Figure 10 shows the system response after 2% initial disturbance in generator rotor speed at $\mu = H \approx 0.401525$ when the nonlinear (cubic) controller is applied.

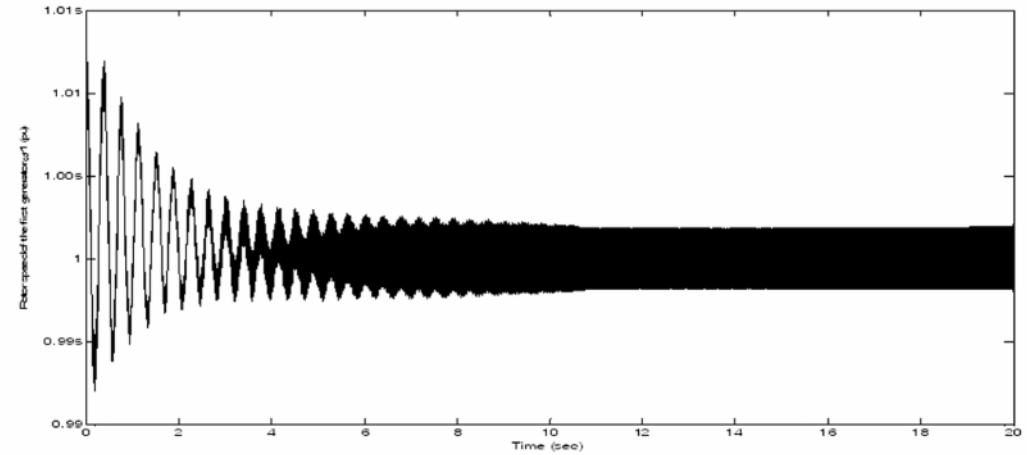

Figure 9: Rotor Speed of the First Generator at $\mu = H \approx 0.401525$ with 2% Initial Disturbance in Rotor Speed of Generator (for the Case of Adding Nonlinear (Quadratic) Controller).

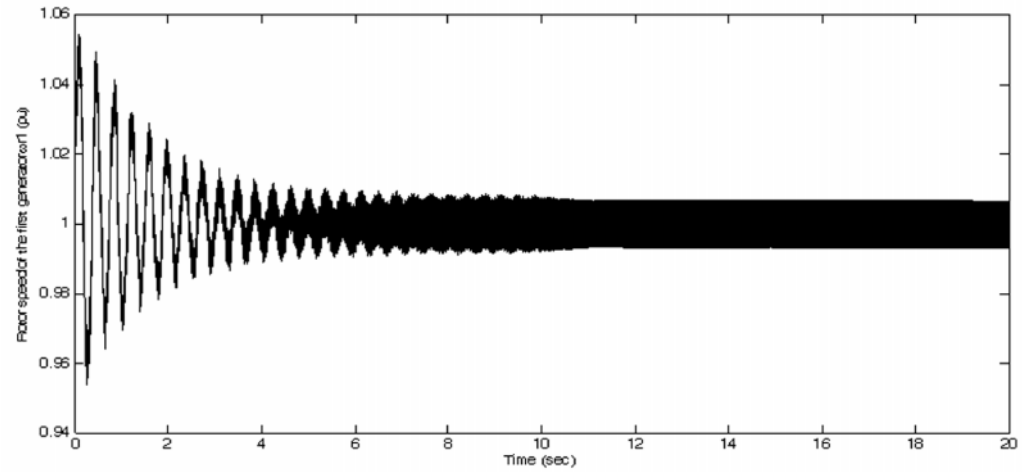

Figure 10: Rotor Speed of the First Generator at $\mu = H \approx 0.401525$ with 2% Initial Disturbance in Rotor Speed of Generator (for the Case of Adding Nonlinear (Cubic) Controller).

6. CONCLUSIONS

Bifurcation theory is applied to the second system of the IEEE second benchmark model of SSR to investigate the complex dynamics of the system. The case of adding damper windings, AVR and PSS is considered. The results show that as the compensation factor ($\mu = X_c / X_L$) increases the operating point loses stability via Hopf bifurcation point. Also, the results showed that the type of this Hopf bifurcation is subcritical. Nonlinear controllers are used to control the Hopf bifurcation and chaos. The results show that nonlinear controller can alter the subcritical Hopf bifurcation to supercritical (that is stabilizing the periodic solution). We start with a

nonlinear controller based on the nonlinearity of the system and by using trial and error criterion. Then Based on bifurcation theory and center manifold theory, nonlinear controllers are used to control a Hopf bifurcation and chaos. Still, either of these controllers can be used to stabilize the system.

REFERENCES

[1] E. H. Abed, "Bifurcation-Theoretic Issues in the Control of Voltage Collapse," *in Proc. IMA Workshop on Systems and Control Theory for Power Systems eds*, J. H. Chow, P. V. Kokotovic and R. J. Thomas (Springer), 1995, pp. 1-21.

[2] D. Chen, H. O. Wang and G. Chen, "Anti-Control of Hopf Bifurcations Through Washout Filter," *Proc. 37th IEEE Conf. Decision and Control*, Tampa, FL, Dec. 16-18, 1998, pp. 3040-3045.

[3] A. Tesi, E. H. Abed, R. Genesio and H.O. Wang, "Harmonic Balance Analysis of Period-Doubling Bifurcations with Implications for Control of Nonlinear Dynamics," *Automatica*, **32**, 1996, pp. 1255-1271.

[4] H. O. Wang and E. H. Abed, "Bifurcation Control of a Chaotic Systems," *Automatica*, **31**, 1995, pp. 1213-1226.

[5] E. H. Abed and J. H. Fu, "Local Feedback Stabilization and Bifurcation Control, I. Hopf Bifurcation," *Syst. Control Lett.*, **7**, 1986, pp. 11-17.

[6] M. J. Laufenberg, M. A. Pai and K. R. Padiyar, "Hopf Bifurcation Control in Power Systems with Static VAR Compensator," *Int. J. Elect. Power and Energy Syst.*, **19**, 1997, pp. 339-347.

[7] G. Chen and X. Dong, "From Chaos to Order: Methodologies, Perspectives and Applications," *World Scientific*, Singapore, 1998.

[8] J. L. Moiola and G. Chen, "Hopf Bifurcation Analysis: A Frequency Domain Approach," *World Scientific*, Singapore, 1996.

[9] M. Basso, A. Evangelisti, R. Genesio and A. Tesi, "On Bifurcation Control in Time Delay Feedback Systems," *Int. J. Bifurcation and Chaos*, **8**, 1998, pp. 713-721.

[10] G. Calandrini, E. Paolini, J. L. Moiola and G. Chen, "Controlling Limit Cycles and Bifurcations," *in Controlling Chaos and Bifurcations in Engineering Systems*, ed. G. Chen (CRC Press), 1999, pp. 200-227.

[11] D. W. Berns, J. L. Moiola and G. Chen, "Feedback Control of Limit Cycle Amplitude from a Fequency Domain Approach," *Automatica*, **34**, 1998, pp. 1567-1573.

[12] U. Cam and H. Kuntman, "A New CCII-Based Sinusoidal Oscillator Providing Fully Independent Control of Oscillation Condition and Frequency." *Microelectron. J.*, **29**, 1998, pp. 913-919.

[13] M. A. Tomim, A. C. Zambroni de Souza, P. P. Carvalho Mendes, and G. Lambert-Torres, "Identification of Hopf Bifurcation in Power Systems Susceptible to Subsynchronous Resonance", *IEEE Bologna Power Tech Conference*, June 23-26, 2003, Bologna, Italy.

[14] E. H. Abed and J. H. Fu, "Local Feedback Stabilization and Bifurcation Control, I. Hopf Bifurcation", *Syst. Control Lett.*, **7**, 1986, pp. 11-17.

[15] E. H. Abed and J. H. Fu, "Local Feedback Stabilization and Bifurcation Control, II. Stationary Bifurcation", *Syst. Control Lett.*, **8**, 1987, pp. 467-473.

[16] A. H. Nayfeh, A. M. Harb, and C-M. Chin, "Bifurcations in Power System Model", *Int. J. Bifurcation and Chaos*, **6**, No. 3, pp. 497-512, 1996.

[17] Seyed A. Shahrestani and David J. Hill, "Control of Nonlinear Bifurcating Systems," the University of Sydney, NSW 2006.

[18] A. H. Nayfeh and B. Balachandran, *Applied Nonlinear Dynamics*, Wiley, New York, 1995.

[19] IEEE SSR Working Group, "Second Benchmark Model for Computer Simulation of Subsynchronous Resonance", *IEEE Trans. on Power Apparatus and Systems*, **PAS- 104**, No.5, 1057-1064, May 1985.

[20] M. M. Alomari and B. S. Rodanski, "The Effects of Machine Components on Bifurcation and Chaos as Applied to Multimachine System", *Topics on Chaotic Systems*, Selected Papers from CHAOS 2008 International Conference. Chania, Crete, Greece, 3-6 June 2008. Edited by: Christos H Skiadas, Ioannis Dimotikalis and Charilaos Skiadas. World Scientific, May 2009.

[21] K. R. Padiyar, M. K. Geetha and K. U. Rao, "A Novel Power Flow Controller for Controlled Series Compensation", *IEE, AC and DC Power Transmission*, 29 April-3 May, Conference Publication No. 423, pp. 329-334, 1996.

[22] A. H. Nayfeh, A. M. Harb and C-M. Chin, "Bifurcation and Chaos in a Power System Model", *Proceedings of the IEEE International Symposium on Circuits and Systems*, ISCAS, Seattle, Washington, April 29- May 3, 1995.

[23] J. Guckenheimer and P. Holmes, *Nonlinear Oscillations, Dynamical Systems, and Bifurcations of Vector Fields*, 3rd ed. New York, NY: Springer –Verlag, 1990.